



Influence of hydrodynamic connectivity on the genetic structure and gene flow of the common pandora *Pagellus erythrinus*

Anna Rita Rossi, Paolo Colangelo, L. Berline, Elisa Angiulli, Giandomenico Ardizzone, Chiheb Fassatoui, Luciana Sola

► To cite this version:

Anna Rita Rossi, Paolo Colangelo, L. Berline, Elisa Angiulli, Giandomenico Ardizzone, et al.. Influence of hydrodynamic connectivity on the genetic structure and gene flow of the common pandora *Pagellus erythrinus*. *Hydrobiologia*, 2019, 834 (1), pp.103-117. 10.1007/s10750-019-3914-y . hal-03016156

HAL Id: hal-03016156

<https://hal.science/hal-03016156>

Submitted on 20 Nov 2020

HAL is a multi-disciplinary open access archive for the deposit and dissemination of scientific research documents, whether they are published or not. The documents may come from teaching and research institutions in France or abroad, or from public or private research centers.

L'archive ouverte pluridisciplinaire **HAL**, est destinée au dépôt et à la diffusion de documents scientifiques de niveau recherche, publiés ou non, émanant des établissements d'enseignement et de recherche français ou étrangers, des laboratoires publics ou privés.

1 **Influence of hydrodynamic connectivity on the genetic structure and**
2 **gene flow of the common pandora *Pagellus erythrinus***

3
4 Anna Rita Rossi¹, Paolo Colangelo^{1, 5,*}, Léo Berline², Elisa Angiulli¹,

5 Giandomenico Ardizzone³, Chiheb Fassatoui⁴, Luciana Sola¹

6

7 ¹ Department of Biology and Biotechnology “C. Darwin”, Sapienza University of Rome,
8 via Borelli 50, 00161 Rome, Italy

9 ² Aix-Marseille Univ, Univ Toulon, CNRS, IRD, MIO UM 110, Mediterranean Institute of
10 Oceanography, Marseille, France

11 ³ Department of Environmental Biology, Sapienza University of Rome, viale
12 dell’Università 32, 00185 Rome, Italy

13 ⁴ Ecosystems and Aquatic Resources Research Unit (UR13AGRO1), National Agronomy
14 Institute of Tunisia (INAT), University of Carthage, Charles Nicolle Avenue 43, 1082
15 Tunis, Tunisia

16 ⁵ National Research Council, CNR-IRET, Via Salaria km 29.300, 00015 Monterotondo
17 (Rome), Italy.

18

19 *** Corresponding author:**

20 Paolo Colangelo

21 National Research Council, Via Salaria km 29.300, 00015 Monterotondo (Rome), Italy.

22 c/o

23 Department of Biology and Biotechnology “C. Darwin”, Sapienza University of Rome, via
24 Borelli 50, 00161 Rome, Italy

25 e-mail: paolo.colangelo@uniroma1.it

26 Telephone: +390649918122

27 Fax: +39 06 4457516

28

29 **Running title:** Genetic structure of common pandora

30 **ABSTRACT**

31 Many marine organisms have complex genetic patterns that cannot be easily
32 resolved by data analysis on spatial distribution of variability usually
33 applied in population genetic studies. We propose an analytical framework
34 to evaluate the role of dispersal during early life stages that considers the
35 actual hydrodynamic connectivity in the Mediterranean Sea, as a factor
36 shaping the population structure of demersal fishes. To this purpose, and to
37 test different scenarios of gene flow, genotypes of individuals of *Pagellus*
38 *erythrinus* sampled at 12 sites in the central Mediterranean Sea were
39 analyzed at ten microsatellite loci. The results show the lack of genetic
40 structure in western Mediterranean basin and a pattern of gene flow that
41 deviates from an isolation by distance model. The observed gene flow
42 estimates appear to be scale-dependent. At local scale, it is likely the result
43 of multifactorial components whereas at a larger scale it is mainly driven by
44 the sea currents, directly influencing dispersal of larvae between sites not
45 reachable by adult movements. Our results stress the importance of a
46 quantitative analysis of potential early life stage dispersal in any study
47 focusing on the population structure of fishes with a long larval stage.

48

49 **KEYWORDS:** demersal, dispersal, marine fishes, microsatellite, Sparidae,
50 oceanic circulation

51 INTRODUCTION

52 Because of the absence of evident and pronounced physical barriers, the
53 marine environment has long been considered an open environment with
54 high potential species dispersal that prevents population subdivision (Hauser
55 & Carvalho, 2008). However, many studies have provided evidence
56 contrary to this hypothesis, i.e. the existence of pronounced population
57 structures even on a limited spatial scale in vagile species (Knutsen et al.,
58 2003; Ovenden et al., 2004; Palero et al., 2008; Ciannelli et al., 2010),
59 indicating a substantial gap between expectation and observation in marine
60 population genetics (Hedgecock & Pudovkin, 2011). Indeed, both biotic
61 (including dispersal ability in different life stages, i.e. adults, juveniles,
62 larvae and eggs) and abiotic (historical and oceanographic) factors
63 components contribute to shape the genetic structure of marine species.
64 Among the biotic factors that are related to dispersal ability, the existence of
65 a pelagic larval phase is considered to play a key role in population
66 connectivity and to be the primary dispersal phase in benthic, demersal and
67 most coastal marine species (Cowen & Sponaugle, 2009). As an example
68 planktonic larval duration (PLD), i.e. the amount of time that pelagic larvae
69 spend in the open sea before settlement, was supposed to be a good
70 predictor of the species' population connectivity and structure. However
71 discordant results were obtained among taxa when this hypothesis was
72 tested (see Bohonak, 1999; Jones et al., 2009; Weersing & Toonen, 2009;
73 Kelly & Palumbi, 2010; Riginos et al., 2011; Modica et al., 2017; Nanninga
74 & Manica, 2018).

75 These evidences, and the absence of correlation between
76 PDL/dispersal/genetic structure in multispecies studies reveals the

77 complexity of the factors affecting population connectivity. Weersing &
78 Toonen (2009) suggested that “larval biology of individual species, not
79 PLD, is likely the primary determinant of realized dispersal”. This is
80 congruent with the idea that factors other than PLD drive population
81 connectivity (Félix-Hackradt et al., 2013) and define the distribution range
82 of fishes (Macpherson & Raventos, 2006; Robitzch et al., 2016; Faillettaz et
83 al., 2018). As an example, within the Mediterranean Sea the effect of
84 oceanographic discontinuities, like currents and fronts, on genetic
85 differentiation is not homogenous on different species, and depends on their
86 life history traits (Pascual et al., 2017). Even more, in coral reef species,
87 larval biology is crucial in connectivity; it determines both the high
88 percentages of local self-recruitment (Swearer et al., 1999; Almany et al.,
89 2007), or the high levels of genetic connectivity across large geographic
90 scales (Horne et al., 2013; Simpson et al., 2014).

91 As far as the abiotic factors are concerned, oceanographic processes (often
92 not properly considered in studies on fish population genetics) can greatly
93 influence, or even determine, the connectivity of marine populations (White
94 et al., 2010; Schunter et al., 2011; Simpson et al., 2014). Therefore,
95 quantitative analyses of hydrodynamic connectivity, i.e. the exchange of
96 particles due to coastal and oceanic circulations at different spatial and
97 temporal scales, may represent a useful framework to interpret the current
98 genetic exchange patterns of a given species (Mitarai et al., 2009; White et
99 al., 2010; Berline et al., 2014). This, in turn, can provide useful information
100 to optimize management of commercially important fishes (Berry et al.,
101 2012).

102 To date, a number of studies have effectively incorporated hydrodynamic
103 connectivity in population genetic research on various marine organisms,
104 using hydrodynamic models as proxy of passive dispersal. On this base
105 different models of seascape connectivity have been developed with the
106 main aims to (a) correlate historical and contemporary patterns of dispersal
107 among populations (see Riginos & Liggins, 2013 for a review), (b)
108 recognize common patterns related both to egg type, larval features and
109 dispersal pathways (White et al., 2010; Crandall et al., 2012; Liggins et al.,
110 2016; Faillettaz et al., 2018), and (c) identify the biological and physical
111 drivers that shape genetic diversity (Simpson et al., 2014; Davies et al.,
112 2015; Liggins et al., 2016). These studies suggested that, at ecological time
113 scales, larval dispersal can show high variance and probably cover smaller
114 spatial scales than reported (Crandall et al., 2012) and that, in co-distributed
115 reef fishes, seascape features are better predictors of spatial genetic patterns
116 than dispersal traits (Liggins et al., 2016). Despite the application of a
117 variety of approaches (Jones et al., 2009), marine dispersal kernels remain
118 still largely undescribed. Here we tested the role of hydrodynamic
119 connectivity - (with different scenarios of gene flow) in determining the
120 observed pattern of the population genetic structure of a demersal fish, the
121 common pandora *Pagellus erythrinus* L. 1758.

122 The common pandora is a commercially important benthopelagic sparid fish
123 that inhabits inshore waters of the continental shelf of the northeastern
124 Atlantic Ocean, from Norway to Guinea-Bissau, and the Mediterranean and
125 Black Sea (Bauchot & Hureau, 1986); it is present up to 200-300 m but
126 most commonly at 20-100 m and occasionally at 100-200 m (Busalacchi et
127 al., 2014). No catch in the 200-800 m stratum has been reported by the

128 international bottom trawl survey in the Mediterranean (MEDITS, 2001).

129 The common pandora is a protogynous hermaphroditic fish that reproduces

130 during late spring and summer (Valdés et al., 2004), when adults migrate

131 from coastal waters to spawn in the open sea; trophic migration, in the

132 opposite direction, occurs in summer-autumn (Županović & Jardas, 1989).

133 Eggs and larvae are pelagic; the median larval stage lasts 44 days and larvae

134 are distributed offshore (>1 mile) (Macpherson & Raventos, 2006). The

135 species has a high commercial value and its catch has increased in the last

136 30 years, particularly along the North African coast of the Mediterranean

137 Sea (FAO, 2018). It is also a candidate for marine fish aquaculture in the

138 Mediterranean Sea, and a small-scale production already exists in Greece

139 (Klaoudatos et al., 2004).

140 Previous mtDNA data (Angiulli et al., 2016) identified three sympatric

141 mitochondrial lineages in specimens collected at 15 sites in the

142 Mediterranean Sea and one in the Atlantic Ocean. The three lineages

143 probably originated from isolation and divergence processes and then came

144 into secondary contact during the Middle and Late Pleistocene glacial and

145 interglacial cycling (Angiulli et al., 2016). Within the central Mediterranean

146 Sea, their distribution does not show any evident geographic pattern,

147 suggesting high connectivity even across the putative boundaries between

148 the biogeographic sectors proposed in the investigated area (Villamor et al.,

149 2014), and between the two Tunisian sites where previous gene enzyme

150 electrophoresis analyses reported genetic differentiation (Fassatoui et al.,

151 2009, 2011). The frequency distribution of mtDNA lineages across sampling

152 sites suggested a more limited matrilinear gene flow only between the

153 Mediterranean Sea and the Atlantic Ocean.

154 According to the idea that nuclear loci should usually provide greater
155 resolution of genetic structure than mtDNA (Angers & Bernatchez, 1998),
156 the main goal of this study was to analyze the present fine-scale population
157 structure and connectivity of *P. erythrinus* within the Mediterranean Sea and
158 to clarify the contribution of dispersal at different life history stages to
159 delineate this structure. For this purpose, we analyzed the genetic variation
160 at 10 microsatellite loci screened in specimens collected at 12 of the 16
161 sampling sites examined by mtDNA analysis (Angiulli et al., 2016). We
162 focused on the Italian and Tunisian sites and estimated the hydrodynamic
163 connectivity in the central Mediterranean Sea using a Lagrangian approach.
164 We assumed that (a) adult common pandora occupy bottoms of the
165 continental platform and are likely unable to move between sites separated
166 by deep stretches of sea, implying that their possible migration routes are
167 limited by the depth; (b) that eggs and larvae occupy superficial waters, as
168 larvae of Sparidae in the Mediterranean Sea are mainly concentrated in the
169 upper 10 m of the water column (Sabatés and Olivar, 1996). Thus, when
170 connectivity exists between two sites separated by a deep stretch of sea (>
171 300 m in depth), we might expect that it is due to pelagic larval migration of
172 early life history stages.

173 With this premise and on the base of the information derived from a
174 Lagrangian model of hydrodynamic connectivity, we tested different gene
175 flow scenarios in a Bayesian framework. In this way we aimed to determine
176 whether the identified genetic structure (i) can be attributed mainly to the
177 active dispersal capabilities of adults or (ii) is mainly shaped by early life
178 history dispersal between pairs of sites due to the effects of hydrodynamic
179 connectivity, or (iii) might be the result of both.

180

181

182 MATERIALS AND METHODS

183

184 Sampling and microsatellite genotyping

185 Common pandora adults (Standard Length > 13 cm) were collected from 12
186 sites along the Italian and Tunisian coasts in the Mediterranean Sea (Table 1,
187 Fig 1). The samples were collected during MEDITS (Mediterranean
188 International Trawl Survey, Bertrand et al., 2002) fishery research surveys
189 or were obtained from commercial fishing landings.

190 Pectoral fin clips were removed and preserved in 96% ethanol at 4°C.

191 Voucher specimens were deposited in the Ichthyology Collection of the

192 Department of Biology and Biotechnology of Sapienza University of Rome

193 (ICDBB 970-974). Genomic DNA was extracted according to the procedure

194 of Aljanabi & Martinez (1997) and then used as a template in polymerase

195 chain reactions (PCR) for 10 microsatellite loci expressly isolated for

196 *Pagellus erythrinus* (MS2, MS3, MS4, MS6, Ramsak et al., 2003) or for

197 other sparids (SL7, SL17, SL26, SL29 and SL33, Chopelet et al., 2009;

198 PbOviD102, Piñera et al., 2006). Loci were amplified in two multiplex

199 reactions in a total volume of 10 µl containing 1 µl of 10x buffer, 0.3 µl of

200 MgCl₂ (50 mM), 0.2 µl of dNTP (2.5 mM), 0.1 µl of each primer (100 µM),

201 0.07 µl of BIOTAQTM DNA polymerase and 10-100 ng of DNA template.

202 The PCRs were performed in a Thermocycler T1 (Biometra, Göttingen,

203 Germany) with an initial denaturation of 2 min at 94°C, followed by 40

204 cycles of 94°C for 30 s, a locus-specific annealing temperature (for each

205 primer as described by the above-mentioned authors) for 45 s and 72°C for

206 30 s and a final extension at 72°C for 5 min. PCR products were run on
207 6.5% denaturing polyacrylamide gel using a LI-COR DNA 4200 automated
208 sequencer (LI-COR Biosciences, Cambridge, UK). Allele sizes were
209 screened using GENE-IMAGE v4.05 software (Scanalytics, Fairfax, VA,
210 USA). Approximately 10% of the samples (50 individuals) were re-scored at
211 all 10 microsatellite loci to ensure repeatability.

212

213 **Data analysis**

214 **Genetic variability and differentiation**

215 Allele frequencies, expected and observed heterozygosity (H_{exp} and H_{obs}),
216 average number of alleles (A), number of private alleles (N_P) and allelic
217 richness (A_R) were estimated per locus and per sampling site using
218 GENEPOP v3.4 (Raymond & Rousset, 1995) and FSTAT v2.9.3.2 (Goudet,
219 2001) software. Deviation from Hardy-Weinberg equilibrium (HWE) and
220 linkage disequilibrium were tested for each locus and pairs of loci
221 respectively, and for sampling site. Statistical significance of both analyses
222 was calculated with the Markov Chain Monte Carlo (MCMC) method using
223 10^4 permutations, 5×10^3 dememorization steps and 500 batches. Sequential
224 false discovery rate (FDR) correction for multiple tests was applied for the
225 HWE tests and for the linkage disequilibrium significance because of the
226 large number of tests involved (Benjamini & Hochberg, 1995).

227 The occurrence of putative null alleles, large allele drop-out and scoring
228 errors was evaluated using MICROCHECKER (Van Oosterhout et al.,
229 2004). Moreover, the frequency of null alleles was tested using the
230 Expectation Maximization algorithm of Dempster et al., (1977),
231 implemented in FreeNA software (Chapuis & Estoup, 2007).

232 The presence of loci under selection was evaluated by the coalescent
233 approach (Beaumont & Nichols, 1996) and by both a global outlier test,
234 implemented in LOSITAN (Antao et al., 2008), and the hierarchical method
235 of Excoffier et al. (2009), using the software ARLEQUIN v3.5 (Excoffier &
236 Lischer, 2010). The LOSITAN analyses were performed under the infinite
237 allele model (IAM) and the stepwise mutation model (SMM) with 95×10^3
238 permutations and 99% confidence interval, while the ARLEQUIN analyses
239 were carried out under a hierarchical island model with 5×10^4 coalescent
240 simulations.

241 Genetic differentiation between samples was tested by F_{ST} (Weir &
242 Cockerham, 1984) and R_{ST} (Slatkin, 1995) using ARLEQUIN v3.5 and
243 RSTCALC v2.1 (Goodman, 1997) respectively, and the significance of
244 pairwise values was calculated with the MCMC method using 10^4
245 permutations, 5×10^3 dememorization steps and 500 batches. Sequential false
246 discovery rate (FDR) correction for multiple tests was applied.

247 The simulation-based program POWSIM v4.1 (Ryman & Palm, 2006) was
248 used to assess the statistical power of the 10 microsatellite loci to detect
249 various levels of divergence among sampling sites. The simulations were
250 performed using different combinations of N_e (effective population size) and
251 t (time of divergence) leading to F_{ST} values in the range 0.005-0.010. The
252 tested values of F_{ST} and N_e were selected according to the estimated values
253 from data of this study (see Results section). The statistical power of the
254 dataset was evaluated using Chi-squared and Fisher's exact tests. The
255 estimate of power was reported as the proportion of significant outcomes
256 ($p < 0.05$) after 1000 replicates.

257 The correlation between least cost geographic distances and the genetic

258 distances, calculated as the $F_{ST}/(1 - F_{ST})$, was analyzed with a Mantel test,
259 using the software R statistical environment (R Development Core Team,
260 2011). Least cost distances among pairs of sites were calculated using the
261 function shortest Path implemented in the “*gdistance*” package (van Etten,
262 2017). In order to obtain a least cost distance, we allowed connection only
263 through areas covered by sea, preventing connection across a land surface.

264

265 **Cluster analysis**

266 Bayesian cluster analysis implemented in STRUCTURE 2.3 (Pritchard et
267 al., 2000) was used to estimate the number of genetic clusters (K) within the
268 dataset. Mean and variance of log likelihoods of the number of clusters for
269 $K=1$ to $K=12$ (the number of sampling sites) were inferred from multilocus
270 genotypes using the MCMC method. Twenty replicates for each set of
271 values of K with 1.5×10^6 iterations (burn-in period of 1×10^5 iterations) were
272 performed under the admixture ancestry model and the assumption of
273 correlated allele frequencies among samples (Falush et al., 2003).

274 In addition to STRUCTURE, discriminant analysis of principal components
275 (DAPC; Jombart et al., 2010) was used to detect the best number of genetic
276 clusters using the function find.cluster. The correct number of clusters (K)
277 was determined by testing K values from 1 to 12. Different clustering
278 solutions were then compared using Bayesian Information Criterion (BIC).
279 Subsequently DAPC was performed (the first 100 PC scores, which account
280 for 80% of the total cumulative variance, were retained) to evaluate the
281 percentage of posterior correct assignments. Both K-means and DAPC were
282 implemented in the R package adegenet v1.3-1 (Jombart, 2008; Jombart &
283 Ahmed , 2011).

284

285 **Hydrodynamic model**

286 A Lagrangian approach was used to quantify hydrodynamic connectivity.
287 We define Oceanic distances (OD) as the mean connection time (MCT)
288 taken by particles to connect two sites. The dispersal of a large ensemble of
289 passive particles by the oceanic circulation was modeled using currents
290 from a multiannual realistic ocean model simulation covering the whole
291 Mediterranean basin. Particles were released in the surface layer (0-100 m)
292 where eggs and larvae are generally found (Klimogianni et al., 2004 and
293 references therein). For each pair of square sub-regions of 50 km per side,
294 the time needed to go from one sub-region to the other (by the particles) was
295 computed. The average time to connect site pairs found in a specific sub-
296 region provides a measure of the oceanic distance. The resulting MCT
297 matrix is asymmetric since the time required by a particle to go from site
298 “a” to site “b” is not equal to the time to go from “b” to “a”. Details of the
299 method and how to calculate MCT can be found in Berline et al. (2014).
300 Here we only consider MCT below 200 days, a time window that includes
301 the embryonic and larval phases as well as the early juvenile stage. The
302 pairwise hydrodynamic connectivity was then used to propose different
303 dispersal scenarios of gene flow (see below).

304

305 **Gene flow and hydrodynamic connectivity**

306 Gene flow within the Mediterranean Sea was estimated using a coalescent
307 based approach implemented in MIGRATE-N v3.6 (Beerli & Felsenstein,
308 2001; Beerli, 2006), and alternative migration hypotheses (Beerli &
309 Palczewski, 2010) were tested.

310 Complete panmixia (Fig. 2, Model 0: all the sampled specimens belong to a
311 unique large panmictic unit) was tested versus seven alternative migration
312 models (Fig. 2, Models 1-7). The evaluated scenarios allowed us to test
313 alternative population structures and migration dynamics (adults and early
314 life history dispersal) along different routes.

315 In the first migration model (Fig. 2: Model 1), sampled populations were
316 pooled according to their geographic sea origin: Ligurian Sea, Tyrrhenian
317 Sea, Sea of Sardinia, Sicilian Channel, Ionian Sea, Adriatic Sea. Migration
318 rates were allowed to be bi-directional between pairs of adjacent seas. All
319 the successive models considered the sampled geographic populations as
320 distinct genetic units, whereas migration rates among them were evaluated
321 according to different schemes. Indeed, in the second migration model (Fig.
322 2: Model 2) the gene flow was considered a bi-directional stepping stone
323 process related to active dispersal of *P. erythrinus*. Thus, the gene flow was
324 estimated only between sites whose distances and path could be covered by
325 adult migration routes along coastlines or across sea stretches less than 300
326 m deep.

327 This model allowed us to identify three groups of sites that can exchange
328 migrants (Fig. 2: Model 2). In the subsequent model (Fig. 2: Model 3) we
329 extended the previous model by considering additional early life history
330 dispersal routes mediated by sea currents. On the basis of oceanic distances
331 (see hydrodynamic connectivity) we identified two routes that allowed us to
332 connect the three groups of Model 2, thus allowing a potential continuous
333 exchange of genes across the sampled sites. In more detail we identified the
334 two unidirectional routes (EN->SN and AL->BZ) that allowed an early life
335 history dispersal between the three groups of units with the shortest period

(112 and 91 days respectively). These migration routes, identified on the basis of the oceanic distances, are congruent with the oceanic circulation known for the area (I.I.M., 1982; Millot & Taupier-Letage, 2005; Berline et al., 2014). In Models 4, 5 and 6 (Fig. 2) only a main effect of early life history gene flow, mediated by oceanic circulation, was considered. In these three models, different thresholds were used to calculate which localities are connected by sea currents respectively up to 100, 150 and 200 days. In these models, migration routes could be uni-directional because in some cases the adopted time thresholds allowed a particle to go from one locality to another but not vice versa. Finally, a further model (Fig. 2: Model 7) was tested considering all the sampled populations as independent genetic units; bi-directional migration was possible among all pairs of sampling sites.

Initially, a number of preliminary runs, using all sites and assuming a full migration matrix, was performed to identify the best parameters for the search. Identification of the optimal MCMC parameters was done until consecutive runs produced overlapping results and the estimated values for all the parameters showed a normal distribution (i.e. no double peaks and narrow intervals). The search parameters were then adopted for all the models tested. Initial migration (M) parameters were estimated using F_{ST} . Default MIGRATE-N priors were used for all the models. For each model two independent multiple MCMCs were run for 1000000 steps, sampling every 100 steps. For each MCMC chain the first 10000 trees were discarded and a static heating scheme was adopted (4 chains with temperatures: 1000000, 3, 1.20, 1). For each analysis the effective sample size (ESS) was evaluated and it was found to be much higher than 1000 for all the parameters in all the models tested, with the only exception for the most

362 complex model (n=144 parameters) showing seven parameters with an ESS
363 slightly lower than 1000. The marginal likelihood of each model, as
364 obtained by Bezier approximation, was used to calculate the model
365 probability, estimated by dividing each marginal likelihood by the sum of
366 the marginal likelihoods of all used models.

367

368 **RESULTS**

369 In total, 470 common pandora individuals from 12 sampling sites (Table 1)
370 were screened for 10 microsatellite loci. The 50 DNA samples that were
371 amplified and scored twice produced identical results in each trial.

372

373 **Genetic variability**

374 Genetic variability parameters vary considerably among the 10 loci (Online
375 resource 1): MS6 is the locus with the lowest number of alleles (14 distinct
376 alleles, $A = 6.4$), while MS2 is the most variable (83 distinct alleles,
377 $A = 35.6$). Private alleles (65) constitute 14% of the total alleles (464),
378 ranging from 7.8% at locus SL17 to 35.3% at locus SL33. The number of
379 alleles per sampling site is medium/high and quite homogeneously
380 distributed across samples (A ranges from 22 to 25.4, Table 1). Private
381 allele distribution across sites ranges from 0.42% at sampling site LM to
382 3.75% at AN. Levels of mean H_{obs} are similar among all samples, ranging
383 from 0.748 to 0.802, but lower than the H_{exp} (Table 1).

384 Significant departures from HWE were observed in 50 of 120 locus/site
385 combinations after FDR correction (Online resource 2). MS2 and SL33 are
386 the most affected loci (Online resource 2). All deviations are characterized
387 by heterozygote deficit, and according to MICROCHECKER half of them

388 are associated with the presence of putative null alleles, whose frequencies
389 in each locus are not uniformly distributed across different sampled
390 populations (Online resource 2). According to this, the deviation from HWE
391 due to heterozygote deficit observed in our dataset cannot be simply
392 explained by a widespread presence of null alleles but rather as the result of
393 a combination of factors including other biological processes (e.g.
394 inbreeding and/or the Wahlund effect). Indeed, heterozygote deficit and
395 positive F_{IS} are also observed when data are calculated for each population
396 (data not shown). The different components that act on heterozygote deficit
397 cannot be easily discerned by a multilocus data analysis (Dharmarajan et al.,
398 2013). Carlsson (2008) demonstrated that the occurrence of null alleles
399 could only slightly affect the assignment test and F_{ST} estimation. Moreover,
400 a conservative approach of discarding loci deviating from HWE
401 expectations could eliminate informative markers and thus affect the
402 inferences on biological phenomena derived from the data (Dharmarajan et
403 al., 2013). According to these considerations and to the non-uniform
404 frequency distribution of null alleles across different populations, we
405 retained one of the two most affected loci, MS2, in the analysis; the other
406 one, SL33, was excluded from the genetic structure analysis as it is also
407 under selection (see below).

408 No linkage disequilibrium was detected for each pair of loci (585 pairwise
409 comparisons) by the FDR method.

410

411 **Population structure**

412 The POWSIM analysis showed that the combination of microsatellite loci
413 and sample sizes rendered a statistical power sufficient to detect a low level

414 of differentiation. In fact, about 95% (χ^2) and more than 90% (Fisher's) of
415 the tests where the N_e/t combination led to $F_{ST} = 0.0010$ and 100% (both χ^2
416 and Fisher's) of the tests where N_e/t led to a F_{ST} value of ≥ 0.0025 were
417 statistically significant (Online resource 3). The F_{ST} values were significant
418 for all loci with the exception of PbOviD102. The global outlier test
419 revealed directional selection at one locus, SL33, using both LOSITAN ($p <$
420 0.01) under IAM and SMM models and ARLEQUIN ($p < 0.001$). These
421 results suggested that SL33 is under positive selection, and for this reason
422 this locus was eliminated from subsequent analyses.

423 Multilocus F_{ST} among all samples = 0.00395 ($p < 0.001$). Multilocus pairwise
424 estimates of F_{ST} and R_{ST} are reported in Table 2. Only two pairwise
425 comparisons were found to be significant after FDR correction, AN-BA and
426 GA-BA, for F_{ST} and R_{ST} , respectively.

427 The Mantel test applied to all sampling sites revealed the absence of
428 correlation between genetic distances, expressed as $F_{ST}/(1 - F_{ST})$, and
429 geographic distances ($z = 231132.8$, $p = 0.175$).

430

431

432 **Cluster analysis**

433 Cluster analyses by means of STRUCTURE identified, among the 12 tested
434 K, the greatest posterior probability value at $K = 1$, i.e. a single genetic
435 cluster.

436 In contrast, according to BIC the best number of clusters inferred by the k-
437 means analyses within the Mediterranean Sea sites is four, and DAPC
438 provided $> 0.96\%$ of posterior correct group assignments. The four genetic
439 clusters can be easily distinguished by the first two discriminant axes, and

each includes a different number of individuals (n=112, 110, 93 and 121 respectively for cluster 1, 2, 3 and 4). All four clusters are not related to specific geographic areas and were found at all the sampling sites (Fig. 3, Online resource 4). Frequency of cluster across the twelve sites is not significantly different according to chi-square test ($p=0.08$)

Gene flow and hydrodynamic connectivity

Lagrangian model returns that only 59 possible connections (versus a total of 144 hypothetical ones) can occur within the threshold of 200 days.

The MCTs range between a maximum of 199 days and a minimum of 53 days, with an average of 134 days. Shortest MCT were found between Sardinian (SN-AL) and Tyrrhenian sites (GA-FM, FM-EN) as well as between Jonian and southern Tyrrhenian sites (JO-VM).

As expected, the largest MCTs were found between sites located in different sea basins. For every pair of sites, a strong asymmetry exists between the two directions of transport (Online resource 5).

Among the different migration models, according to the marginal likelihoods, the highest support (relative probability, $P=1$) was obtained for Model 3 (Online resource 6). All the estimated migration rates (M) show narrow 95% confidence intervals with density distributions following a normal distribution. Migration rates between pairs of sites are scattered across a wide range of values and are summarized in Fig. 4a and b. Estimated migration rates are almost symmetrical between all pairs of sites, with the exception of FM \leftrightarrow EN and LM \leftrightarrow ZA (Fig 4a). The estimated migration rates between pairs of sites (EN \rightarrow SN and AL \rightarrow BZ) that cannot be reached by adult *P. erythrinus* are comparable or even higher than those

466 observed between geographically adjacent pairs of sites that can be reached
467 by adult dispersal. Very low migration rates were observed among a few
468 sites and particularly characterized Adriatic (AN, BA) and Ionian (JO) sites.

469

470 **DISCUSSION**

471 **Population structure**

472 Our results highlight a lack of spatial population structure in the common
473 pandora, similar to what observed in other Mediterranean demersal species
474 (Schunter et al., 2011; Franchini et al., 2012). Partial inconsistencies among
475 results obtained by the different analysis/programs employed could derive
476 from the different assumptions on which the various methods rely, such as a
477 priori grouping of individuals or their assumed pure/mixed ancestry. As an
478 example, simulated data show that below $F_{ST} = 0.1$, STRUCTURE is unable
479 to correctly identify the number of subpopulations, providing false certainty
480 regarding the K (Latch et al., 2006).

481 STRUCTURE suggests potential panmixia in the common pandora whereas
482 this scenario, that consider random genetic exchange among individuals and
483 population with the same probability, is rejected by the MIGRATE-N model
484 comparison. The k-means clustering and DAPC methods identify four
485 different genetic clusters (Online resource 4), which however are spread
486 across all sites and thus fail to identify a spatial structuring of genetic
487 diversity. A previous mtDNA sequence analysis of the same samples within
488 the Mediterranean Sea depicted a similar pattern characterized by the
489 absence of a spatial genetic structure (Angiulli et al., 2016). Due to their
490 different mutation rates and uni- or bi-parental inheritance, mitochondrial
491 DNA and microsatellites usually provide different sensitivities at different

temporal scales. Mitochondrial DNA is more suitable to record signatures of historical processes (Avise, 2000), related to the last few million years. Microsatellites perform better in unraveling contemporary and recent processes, i.e. occurring in the last 10 thousand years (Hewitt, 2004). The advance of combining of the two kind of markers has been proved in marine fishes (Limborg et al., 2012), although sometimes they can yield different results, i.e. identify, different numbers of subpopulations (Durand et al., 2013; Lemos et al., 2005; Sala-Bozano et al., 2009; Silva et al., 2014). In the common pandora mtDNA and microsatellites provide similar pattern of genetic diversity with differentiated genetic clusters, occurring in sympatry. This pattern could be explained by group differentiation due to vicariance events, with the groups subsequently entering into secondary contact once the disappearance of putative barriers permitted complete connectivity in the Mediterranean basin.

506

Impact of hydrodynamic connectivity on gene flow pattern

Knowledge of the influence of hydrodynamic patterns on population connectivity of many Mediterranean species is still scarce, whereas it could be particularly important for the study of the genetic structure of demersal fishes. In these species, adults are usually associated with benthonic environments and, although capable of long-distance dispersion, are limited in crossing deep sea stretches, that act as natural barriers. As a consequence, long-range dispersal cannot be attributed to adult movements alone, but rather also to what occurs during the earliest ontogenetic stages, when eggs and larvae are dispersed by sea currents.

We employed an analytical method that allowed us to gain insight into the

518 gene flow and connectivity among common pandora populations. We tested
519 different scenarios in which we assumed a different role of passive and
520 active dispersal in determining the observed population structure in the
521 western Mediterranean Sea. Our model selection approach suggests a
522 scenario in which the gene flow over long distances is due to dispersal of
523 eggs and larvae by oceanic currents, whereas at a small scale can effectively
524 be affected by adult's movement. This scenario agrees with what we know
525 about the biology of this species. Thus, it is likely that gene flow between
526 neighboring sites (on the same coast or connected by a body of water less
527 than 300 m deep) can occur by active movement of adults, even though a
528 contribution by sea currents to the gene flow among neighboring sites
529 cannot be completely ruled out. We tried to determine the potential
530 contribution of adult and larval migration over short distances by assessing
531 the influence of both oceanic and geographic distances on the estimated
532 mean gene flow in the best-supported migration scenario of Model 3.
533 Therefore, our results suggest that over long distances hydrodynamic
534 connectivity and gene flow in the common pandora are affected by dispersal
535 of eggs and larvae, and thus directly by oceanic circulations, gyres and
536 barriers present within the Mediterranean Sea (Limborg et al., 2012). On the
537 other hand, over short distances, it is likely that a mixed contribution by sea
538 currents, adult movements and/or other biophysical phenomena determines
539 the exchange among populations. As an example, recently simulated
540 scenarios on other sparids showed that larval behavior could actually affect
541 connectivity: swimming abilities of just few cm s^{-1} , at the end of the pelagic
542 phase, can impact on the rate of recruitment and change connectivity
543 patterns at regional scale (Faillettaz et al., 2018).

544 All these phenomena act at different scales determining a lack of spatial
545 genetic structure. Further studies are necessary for a generalization of this
546 connectivity pattern to other demersal fishes, but it is important to stress that
547 a similar pattern of genetic structure was reported in the same geographic
548 area for another sparid, the coastal *S. aurata* (Franchini et al., 2012), which
549 has a comparable long-lasting larval stage (about 50 days).
550 Finally, it is important to frame the excess of homozygotes observed in the
551 sampled populations within the gene flow scenario supported by our
552 analyses. Under a scenario of weak population structure and extensive gene
553 flow (as confirmed by F_{ST} and MIGRATE-N analyses), a high proportion of
554 heterozygotes at most of the sampled loci is expected. On the other side, a
555 recent study on the evolutionary consequences of alternative sex change
556 pathways by Benvenuto et al. (2017) demonstrated a reduction of the
557 effective population in protogynous fishes and also reported a reduction of
558 heterozygotes in *P. erythrinus*. Further data indicate that biophysical
559 phenomena can cause a long-term aggregation of larval fish siblings during
560 dispersal, causing a deviation from Hardy-Weinberg proportions in samples
561 containing a high proportion of related individuals (Ottmann et al., 2016).
562 Thus, in *P. erythrinus* the extensive gene flow could be compatible with an
563 excess of homozygotes, considering an effective low number of breeders or
564 other phenomena that allow the passive dispersal of large numbers of
565 siblings.

566

567

568 **Conclusion**

569 A quantitative method that evaluates the effect of hydrodynamic

570 connectivity on gene flow can be a powerful tool for an understanding of the
571 population genetics and dynamics of demersal fishes. Our seascape genetic
572 analyses in the common pandora allowed us to elucidate population
573 dynamics and dispersal patterns, confirming the usefulness of genetic
574 approaches in testing predictions about transport mechanisms in the sea
575 (Selkoe et al., 2016). Our results suggest that gene flow across the central
576 Mediterranean Sea in the common pandora, and likely in other demersal
577 fishes, is extremely complex and driven by a combination of factors acting
578 at different scales, including movements of both adults and eggs and larval
579 migration. The complex pattern detected in the central Mediterranean Sea
580 suggests that in fish population genetic studies, hydrodynamic connectivity
581 estimates can help not only to understand the distribution of genetic
582 diversity but also to study dispersal patterns of demersal fishes. Moreover,
583 clarifying the interactions between hydrodynamic connectivity and
584 population genetics could provide useful information for fisheries
585 management and for the better design of marine protected areas (Andrello et
586 al., 2015)

587

588 **ACKNOWLEDGEMENTS**

589 We thank the MEDITS coordinators and all of our colleagues for their
590 invaluable help with sample collection, specifically Maria Teresa Spedicato
591 and Giuseppe Lembo, COISPA (Bari); Angelo Cau, Dept. of Life and
592 Environmental Sciences, Cagliari University; Corrado Piccinetti, Dept. of
593 Biological, Geological and Environmental Sciences, Bologna University;
594 Angelo Tursi, Dept. of Biology, Bari University; Fabio Fiorentino, Coastal
595 Marine Environment Institute, Mazara del Vallo and Mohamed Salah

596 Romdhane, INAT/Université de Carthage, Tunisia. Financial support for
597 this work was provided by Sapienza University of Rome, Sapienza Projects
598 2014, grant C26A143AL3

600**REFERENCES**

601

602 Aljanabi, S. M. & I. Martinez, 1997. Universal and rapid salt extraction of

603 high quality genomic DNA for PCR-based techniques. *Nucleic Acids*604 *Research* 25:4692–4693.

605 Almany, G. R., M. L. Berumen, S. R. Thorrold, S. Planes & G. P. Jones,

606 2007. Local replenishment of coral reef fish populations in a marine

607 reserve. *Science* 316: 742-744.

608 Andrello, M., M. N. Jacobi, S. Manel, W. Thuiller & D. Mouillot, 2015.

609 Extending networks of protected areas to optimize connectivity and

610 population growth rate. *Ecography* 38:273–282.

611 Angers, B. & L. Bernatchez, 1998. Combined use of SMM and non-SMM

612 methods to infer fine structure and evolutionary history of closely related

613 brook charr (*Salvelinus fontinalis*, Salmonidae) populations from614 microsatellites. *Molecular Biology and Evolution* 15:143–159

615 Angiulli, E., L. Sola, G. Ardizzone, C. Fassatoui & A. R. Rossi, 2016.

616 Phylogeography of the common pandora *Pagellus erythrinus* in the

617 central Mediterranean Sea: sympatric mitochondrial lineages and genetic

618 homogeneity. *Marine Biology Research* 12:4-15.

619 Antao, T., A. Lopes, R. J. Lopes, A. Beja-Pereira & G. Luikart, 2008.

620 LOSITAN: a workbench to detect molecular adaptation based on a *Fst*-621 outlier method. *BMC Bioinformatics* 9:323.622 Avise, J. C., 2000. *Phylogeography. The history and formation of species.*

623 Harvard University Press: Cambridge, MA.

624 Bauchot, M. L. & J. C. Hureau, 1986. Sparidae. In: Whitehead PJP, Bauchot

625 ML, Hureau JC, Nielsen J, Tortonese E (eds), *Fishes of the north-eastern*

626 Atlantic and the Mediterranean, UNESCO, Paris. Vol 2: 883-907.

627 Beaumont, M. A. & R. A. Nichols, 1996. Evaluating loci for use in the
628 genetic analysis of population structure. Proceedings of the Royal
629 Society of London B: Biological Sciences 263:1619-1626.

630 Beerli, P., 2006. Comparison of Bayesian and maximum likelihood
631 inference of population genetic parameters. Bioinformatics 22:341–345.

632 Beerli, P. & J. Felsenstein, 2001. Maximum likelihood estimation of a
633 migration matrix and effective population sizes in n subpopulations by
634 using a coalescent approach. Proceeding of the National Academy of
635 Science USA 98:4563–4568.

636 Beerli, P. & M. Palczewski, 2010. Unified framework to evaluate panmixia
637 and migration direction among multiple sampling locations. Genetics
638 185:313–326

639 Benjamini, Y. & Y. Hochberg, 1995. Controlling the false discovery rate: a
640 practical and powerful approach to multiple testing. Journal of the Royal
641 Statistical Society: Statistical methodology 57: 289–300.

642 Benvenuto, C., I. Coscia, J. Chopelet, M. Sala-Bozano & S. Mariani, 2017.
643 Ecological and evolutionary consequences of alternative sex change
644 pathways in fish. Scientific Reports| 7: 9084

645 Berline, L., A. M. Rammou, A. Doglioli, A. Molcard & A. Petrenko, 2014. A
646 Connectivity-Based Eco-Regionalization Method of the Mediterranean
647 Sea. PLoS ONE 9:e111978.

648 Berry, O., P. England, D. Fairclough, G. Jackson & J. Greenwood, 2012.
649 Microsatellite DNA analysis and hydrodynamic modelling reveal the
650 extent of larval transport and gene flow between management zones in an

651 exploited marine fish (*Glaucosoma hebraicum*). Fisheries Oceanography
652 21: 243-254.

653 Bertrand, J., L. Gil de Sola, C. Papaconstantinou, C. Relini & A.
654 Souplet, 2002. The general specifications of the MEDITS surveys.
655 Scientia Marina 66:9–17.

656 Bohonak, A. J., 1999. Dispersal, gene flow, and population structure. The
657 Quarterly Review of Biology 74: 21-45.

658 Busalacchi, B., T. Bottari, D. Giordano, A. Profeta & P. Rinelli, 2014.
659 Distribution and biological features of the common pandora, *Pagellus*
660 *erythrinus* (Linnaeus, 1758), in the southern Tyrrhenian Sea (Central
661 Mediterranean). Marine Research 68:491–501

662 Carlsson, J., 2008. Effects of microsatellite null alleles on assignment
663 testing. Journal of Heredity 99: 616–623.

664 Chapuis, M. P. & A. Estoup, 2007. Microsatellite null alleles and estimation
665 of population differentiation. Molecular Biology and Evolution 24:621-
666 631.

667 Choquet, J., S. Helyar, B. Mann, & S. Mariani, 2009. Novel polymorphic
668 microsatellite loci for the protogynous hermaphrodite slinger sea bream
669 (*Chrysoblephus puniceus*, Sparidae). Molecular Ecology Research
670 9:1223–1226.

671 Lorenzo Ciannelli, L., H. Knutsen, E. M. Olsen, S. H. Espeland, L. Asplin,
672 A. Jelmert, J. A. Knutsen and N. C. Stenseth, 2010. Small-scale genetic
673 structure in a marine population in relation to water circulation and egg
674 characteristics. Ecology 91: 2918–2930.

675 Cowen, R. & S. Sponaugle, 2009. Larval dispersal and marine population
676 connectivity. Annual Review of Marine Science 1:443–466.

677 Crandall, E. D., E. A. Trembl & P. H. Barber, 2012. Coalescent and
678 biophysical models of stepping-stone gene flow in neritid snails.
679 Molecular Ecology 21: 5579–5598

680 Davies, S. W., E. A. Trembl, C. D. Kenkel & M. V. Matz, 2015. Exploring the
681 role of Micronesian islands in the maintenance of coral genetic diversity
682 in the Pacific Ocean. Molecular Ecology 24: 70–82.

683 Dempster, A. P., N. M. Laird, & D. B. Rubin, 1977. Maximum likelihood
684 from incomplete data via the EM algorithm. Journal of the Royal
685 Statistical Society: Statistical methodology 39:1-38.

686 Dharmarajan, G., W. S. Beatty & E. R. Olin Jr, 2013. Heterozygote
687 deficiencies caused by a Wahlund effect: Dispelling unfounded
688 expectations. The Journal of Wildlife Management 77: 226–234.

689 Durand, J. D., H. Blel, K. N. Shen, E. T. Koutrakis & B. Guinand, 2013.
690 Population genetic structure of *Mugil cephalus* in the Mediterranean and
691 Black Seas: a single mitochondrial clade and many nuclear barriers.
692 Marine Ecology Progress Series 474:243–261.

693 Excoffier, L. & H. E. L. Lischer, 2010. Arlequin suite ver 3.5: a new series of
694 programs to perform population genetics analyses under Linux and
695 Windows. Molecular Ecology Resources 10:564-567.

696 Excoffier, L., T. Hofer & M. Foll, 2009. Detecting loci under selection in a
697 hierarchically structured population. Heredity 103:285–298.

698 Faillettaz, R., C. B. Paris & J. O. Irisson, 2018. Larval fish swimming
699 behavior alters dispersal patterns from marine protected areas in the
700 north-western Mediterranean Sea. Frontiers in Marine Science 5:97.

701 Falush, D., M. Stephens & J. K. Pritchard, 2003. Inference of population
702 structure using multilocus genotype data: linked loci and correlated allele

703 frequencies. Genetics 164:1567–1587.

704 FAO, 2018. FishStat plus. Capture production 1950-2012, Aquaculture
705 production 1950-2016. Available from
706 <http://www.fao.org/fishery/statistics/software/fishstatj/en> Accessed
707 March 2018.

708 Fassatoui, C., E. Mdelgi & M. S. Romdhane, 2009. A preliminary
709 investigation of allozyme genetic variation and population structure in
710 common pandora (*Pagellus erythrinus*, Sparidae) from Tunisian and
711 Libyan coasts. Ichthyological Research 56:301-307.

712 Fassatoui, C., E. Mdelgi & M. S. Romdhane, 2011. Short-term temporal
713 genetic investigation of two populations of *Pagellus erythrinus*
714 (Linnaeus, 1758, Sparidae) from Western and Eastern Mediterranean
715 basins off the Tunisian coast. Marine Biology Research 7:147–158.

716 Faurby, S. P. H. Barber, 2012. Theoretical limits to the correlation between
717 pelagic larval duration and population genetic structure. Molecular
718 Ecology 21: 3419–3432.

719 Félix-Hackradt, F. C., C. W. Hackradt, Á. Pérez-Ruzafa & J. A. García-
720 Charton, 2013. Discordant patterns of genetic connectivity between two
721 sympatric species, *Mullus barbatus* (Linnaeus, 1758) and *Mullus*
722 *surmuletus* (Linnaeus, 1758), in south-western Mediterranean Sea.
723 Marine Environmental Research 92:23-34.

724 Franchini, P., L. Sola, D. Crosetti, V. Milana & A. R. Rossi, 2012. Low
725 levels of population genetic structure in the gilthead seabream, *Sparus*
726 *aurata*, along the Italian coasts. ICES Journal of Marine Science 69:41-
727 50.

728 Galarza, J. A., J. Carreras-Carbonell, E. Macpherson, M. Pascual, S.

729 Roques, G. F. Turner & C. Rico, 2009. The influence of oceanographic
730 fronts and early-life-history traits on connectivity among littoral fish
731 species. *Proceedings of the National Academy of Science USA*
732 106:1473–1478. 6

733 Goodman, S. J., 1997. RSTCALC: A collection of computer programs for
734 calculating unbiased estimates of genetic differentiation and determining
735 their significance for microsatellite data. *Molecular Ecology* 6:881-885.

736 Goudet, J., 2001. FSTAT, a program to estimate and test gene diversities and
737 fixation indices (version 2.9.3). Institute of Ecology, University of
738 Lausanne, Lausanne, Switzerland

739 Hauser, L, & J. R. Carvalho, 2008. Paradigm shifts in marine fisheries
740 genetics: ugly hypotheses slain by beautiful facts. *Fish and Fisheries*
741 9:333–362.

742 Hedgecock, D. & A. Pudovkin, 2011. Sweepstakes reproductive success in
743 highly fecund marine fish and shellfish: a review and commentary.
744 *Bulletin of Marine Science*. 87: 971–1002.

745 Hewitt, G. M., 2004. The structure of biodiversity – insights from molecular
746 phylogeography. *Frontiers in Zoology* 1:4.

747 Horne, J. B., L. van Herwerden, S. Abellana & J. L. McIlwain, 2013.
748 Observations of migrant exchange and mixing in a coral reef fish
749 metapopulation link scales of marine population connectivity. *Journal of*
750 *Heredity* 104: 532–546.

751 I.I.M. Istituto Idrografico della Marina 1982 Atlante delle correnti
752 superficiali dei mari italiani 3068.

753 Jombart, T., 2008. Adegnet: a R package for the multivariate analysis of
754 genetic markers. *Bioinformatics* 24:1403–1405.

755 Jombart, T. & I. Ahmed, 2011. Adegnet 1.3-1: new tools for the analysis of
756 genome-wide SNP data. *Bioinformatics* 27:3070-1.

757 Jombart, T., S. Devillard & F. Balloux, 2010. Discriminant analysis of
758 principal components: a new method for the analysis of genetically
759 structured populations. *BMC Genetics* 11:94.

760 Jones, G. P., G. R. Almany, G. R. Russ, P. F. Sale, R. S. Steneck, M. J. H. van
761 Oppen & B. L. Willis, 2009. Larval retention and connectivity among
762 populations of corals and reef fishes: history, advances and challenges.
763 *Coral Reefs* 28: 307–325.

764 Kelly, R. P. & S. R. Palumbi, 2010. Genetic structure among 50 species of
765 the northeastern Pacific rocky intertidal community. *PLoS One*. 2010 Jan
766 7;5:e8594.

767 Klaoudatos, S. D., G. Iakovopoulos & D. S. Klaoudatos, 2004. *Pagellus*
768 *erythrinus* (common pandora): a promising candidate species for
769 enlarging the diversity of aquaculture production. *Aquaculture*
770 *International* 12:299–320.

771 Klimogianni, A., G. Koumoundouros, P. Kaspiris & M. Kentouri, 2004.
772 Effect of temperature on the egg and yolk-sac larval development of
773 common pandora, *Pagellus erythrinus*. *Marine Biology* 145: 1015–1022.

774 Knutsen, H., P. E. Jorde, C. Andre & N. C. Stenseth, 2003. Fine-scaled
775 geographic population structuring in a highly mobile marine species: the
776 Atlantic cod. *Molecular Ecology* 12:385–39.

777 Latch, E. K., G. Dharmarajan, J. C. Glaubitz & O. E. Rhodes, 2006. Relative
778 performance of Bayesian clustering software for inferring population
779 substructure and individual assignment at low levels of population
780 differentiation. *Conservation Genetics* 7:295–302.

781 Lemos, A., A. I. Freitas, A. T. Fernandes, R. Goncalves, J. Jesus & C.
 782 Andrade, 2006. Microsatellite variability in natural populations of the
 783 blackspot seabream *Pagellus bogaraveo* (Brünnich, 1768): a database to
 784 access parentage assignment in aquaculture. *Aquaculture Research*
 785 37:1028–1033.

786 Liggins, L., E. A. Trem, H.P. Possingham & C. Riginos, 2016. Seascape
 787 features, rather than dispersal traits, predict spatial genetic patterns in co-
 788 distributed reef fishes. *Journal of Biogeography* 43: 256–267.

789 Limborg, M. T., R. Hanel, P. V. Debes, A. K. Ring, C. André, C. S.
 790 Tsigenopoulos & D. Bekkevold, 2012. Imprints from genetic drift and
 791 mutation imply relative divergence times across marine transition zones
 792 in a pan-European small pelagic fish (*Sprattus sprattus*). *Heredity*
 793 109:96-107.

794 Macpherson, E. & N. Raventos, 2006. Relationship between pelagic larval
 795 duration and geographic distribution of Mediterranean littoral fishes.
 796 *Marine Ecology Progress Series* 327:257–265.

797 MEDITS Biological Report 2001 available at
 798 <http://www.sibm.it/SITO%20MEDITS/principaleprogramme.htm>).

799 Millot, C. & I. Taupier-Letage, 2005. Circulation in the Mediterranean Sea.
 800 In: Saliot A (ed.) *The Mediterranean Sea Vol 5k of Handbook of*
 801 *Environmental Chemistry*. Springer: Berlin. p 29–66.

802 Mitarai, S., D. A. Siegel, J. R. Watson, C. Dong, C. & J. C. McWilliams,
 803 2009. Quantifying connectivity in the coastal ocean with application to
 804 the Southern California Bight. *Journal of Geophysical Research* 114:
 805 C10026.

806 Modica, M.V., V. Russini, G. Fassio & M. Oliverio, 2017. Do larval types

807 affect genetic connectivity at sea? Testing hypothesis in two sibling
808 marine gastropods with contrasting larval development. *Marine*
809 *Environmental Research* 127:92–101.

810 Nanninga, G. B. & A. Manica, 2018. Larval swimming capacities affect
811 genetic differentiation and range size in demersal marine fishes. *Marine*
812 *Ecology Progress Series* 589: 1–12.

813 Ovenden, J. R., J. Salini, S. O'Connor & R. Street, 2004. Pronounced
814 genetic population structure in a potentially vagile fish species
815 (*Pristipomoides multidens*, Teleostei; Perciformes; Lutjanidae) from the
816 East Indies triangle. *Molecular Ecology* 13: 1991–1999.

817 Palero, F., P. Abello, E. Macpherson, M. Gristina & M. Pascual, 2008.
818 Phylogeography of the European spiny lobster (*Palinurus elephas*):
819 influence of current oceanographical features and historical processes.
820 *Molecular Phylogenetics and Evolution* 48:708–717.

821 Pascual, M., B. Rives, C. Schunter & E. Macpherson, 2017. Impact of life
822 history traits on gene flow: A multispecies systematic review across
823 oceanographic barriers in the Mediterranean Sea. *PLoS ONE*
824 12:e0176419.

825 Piñera, J. A., D. Bernardo, G. Blanco, E. Vazquez & J. A. Sanchez, 2006.
826 Isolation and characterization of polymorphic microsatellite markers in
827 *Pagellus bogaraveo*, and cross-species amplification in *Sparus aurata*
828 and *Dicentrarchus labrax*. *Molecular Ecology Notes* 6:33–35.

829 Pinet, P. R., 2009. *Invitation to Oceanography*, 5th edn. Jones and Bartlett
830 Publishers, Burlington, MA, USA.

831 Piry, S., G. Luikart & J. M. Cornuet, 1999. BOTTLENECK: a computer
832 program for detecting recent reductions in the effective population size

833 using allele frequency data. *Journal of Heredity* 90:502–503.

834 Pritchard, J. K., M. Stephens, P. Donnelly, 2000. Inference of population
835 structure using multilocus genotype data. *Genetics* 155:945–959.

836 Ramsak, A., F. Garoia, I. Guarniero, P. Mannini & F. Tinti, 2003. Novel
837 polymorphic microsatellite markers for the common pandora (*Pagellus*
838 *erythrinus*). *Molecular Ecology Notes* 3:553–555.

839 Raymond, M. & F. Rousset, 1995. An exact test for population
840 differentiation. *Evolution* 49:1280–1283.

841 R Development Core Team, 2011. R: A language and environment for
842 statistical computing. R Foundation for Statistical Computing, Vienna,
843 Austria ISBN 3-900051-07-0, URL <http://www.R-project.org>

844 Riginos, C., K. E. Douglas, Y. Jin, D. F. Shanahan, & E. A. Trembl, 2011.
845 Effects of geography and life history traits on genetic differentiation in
846 benthic marine fishes. *Ecography* 34: 566–575.

847 Riginos, C. & L. Liggins, 2013. Seascape genetics: populations, individuals,
848 and genes marooned and adrift. *Geography Compass* 7: 197–216.

849 Robitzsch, V. S. N., D. Lozano-Cortés, N. M. Kandler, E. Salas & M. L.
850 Berumen, 2016. Productivity and sea surface temperature are correlated
851 with the pelagic larval duration of damselfishes in the Red Sea. *Marine*
852 *Pollution Bulletin* 105: 566–574.

853 Ryman, N. & S. Palm, 2006. POWSIM: a computer program for assessing
854 statistical power when testing for genetic differentiation. *Molecular*
855 *Ecology Notes* 6:600–602.

856 Sabatés, A. & M. P. Olivar, 1996. Variation of larval fish distributions
857 associated with variability in the location of a shelf-slope front. *Marine*
858 *Ecology Progress Series* 135: 11–20.

859 Sala-Bozano, M., V. Ketmaier & S. Mariani, 2009. Contrasting signals from
860 multiple markers illuminate population connectivity in a marine fish.
861 *Molecular Ecology* 18:4811-4826.

862 Schunter, C., J. Carreras-Carbonell, E. Macpherson, J. Tintore, E. Vidal-
863 Vijande, & A. Guidetti & M. Pascual, 2011. Matching genetics with
864 oceanography: directional gene flow in a Mediterranean fish species.
865 *Molecular Ecology* 20:5167-5181.

866 Selkoe, K. A., K. T. Scribner & H. M. Galindo, 2016. Waterscape Genetics –
867 Applications of landscape genetics to rivers, lakes, and seas. In:
868 Balkenhol N, Cushman SA, Storfer AT, Waits LP (eds) *Landscape*
869 *Genetics - concepts, methods, applications*, Wiley & Sons, Chichester,
870 UK. p 220-246.

871 Silva, G, J. B. Horne & R. Castilho, 2014. Anchovies go north and west
872 without losing diversity: post-glacial range expansions in a small pelagic
873 fish. *Journal of Biogeography* 41:1171–1182.

874 Simpson, S.D., H. B. Harrison, M. R. Claereboudt & S. Planes, 2014. Long-
875 Distance dispersal via ocean currents connects Omani clownfish
876 populations throughout entire species range. *PLoS ONE* 9:e107610.

877 Slatkin, M., 1995. A measure of population subdivision based on
878 microsatellite allele frequencies. *Genetics* 139: 457-462

879 Swearer, S. E., J. E. Caselle, D. W. Lea & R. R. Warner, 1999. Larval
880 retention and recruitment in an island population of a coral-reef fish.
881 *Nature* 402: 799-802.

882 Weersing, K. & R. J. Toonen, 2009. Population genetics, larval dispersal,
883 and connectivity in marine systems. *Marine Ecology Progress Series* 393:
884 1–12.

885 Weir, B. S. & C. C. Cockerham, 1984. Estimating F-statistics for the
 886 analysis of population structure. *Evolution*, 38: 1358–1370

887 White, C., K. A. Selkoe, J. Watson, D. A. Siegel, D. C. Zacher & R. J.
 888 Toonen, 2010. Ocean currents help explain population genetic structure.
 889 *Proceedings of the Royal Society B* 277: 1685-1694.

890 Valdés, P., A. García-Alcázar, I. Abdel, M. Arizcun, C. Suárez & E. Abellán,
 891 2004. Seasonal changes on gonadosomatic index and maturation stages
 892 in common pandora *Pagellus erythrinus* (L.). *Aquaculture International*
 893 12: 333–343.

894 Van Etten J., 2017. R Package gdistance: Distances and Routes on
 895 Geographical Grids. *Journal of Statistical Software* 76: 1-21.

896 Van Oosterhout, C., W. F. Hutchinson, D. P. M. Wills & P. Shipley, 2004.
 897 Micro-checker: software for identifying and correcting genotyping
 898 errors in microsatellite data. *Molecular Ecology Notes* 4: 535–538.

899 Villamor, A., F. Costantini & M. Abbiati, 2014. Genetic Structuring across
 900 marine biogeographic boundaries in rocky shore invertebrates.
 901 *PLoS ONE*, **9**, e101135.

902 Županović, Š. & I. Jardaš, 1989. Fauna i flora Jadrana. Logos Split. 526 pp.
 903
 904

905 **FIGURE LEGENDS**

906

907 **Fig. 1** Fig. 1 Map of the sampling sites of *P. erythrinus*, abbreviated as in
908 Table1. Grey outline indicates the 300m isobath within which *P. erythrinus*
909 adults can actively move and above which they cannot be found.

910

911 **Fig. 2** Different models of population connectivity. Model 0: sampled
912 populations belong to a unique panmictic unit; Model 1-7: populations are
913 pooled according to different criteria or are considered as independent units,
914 and different option of migration are allowed (see text for details).

915

916 **Fig. 3** Frequency distribution of the four clusters identified by discriminant
917 analysis of principal components across sampling sites.

918

919 **Fig. 4** Migration rates between localities according to Model 3. (a) The
920 median estimate is reported (vertical dash) with 50% (bold continuous line)
921 and 95% (dotted line) confidence intervals; (b) Thickness of the arrows is
922 proportional to the mean estimate.

923 **ELECTRONIC SUPPLEMENTARY MATERIAL**

924

925 **Online resource 1** Summary statistics for 10 microsatellite loci over the 12
926 common pandora sampling sites analyzed.

927

928 **Online resource 2** Locus/site combination tests for null alleles (NA; in
929 parentheses their estimated frequencies) and for stuttering errors (ST). In
930 grey, deviations from Hardy-Weinberg expectations.

931

932 **Online resource 3** POWSIM simulations

933

934 **Online resource 4** Discriminant Analysis of Principal Component (DAPC).

935

936 **Online resource 5** Calculated mean connection time (MCT) between pairs
937 of sites

938

939 **Online resource 6** Comparison of the eight models. For each model, the
940 marginal likelihood estimated using the Bezier approximation is reported.

941 **Table 1** Details for sampling and summary statistics over ten loci. N: number of individuals,
942 A: average number of alleles, N_P: number of private alleles, H_{exp}: mean expected
943 heterozygosity, H_{obs}: mean observed heterozygosity, Fis: inbreeding coefficient (all the
944 values are significant for p<0.0001).

Sea	Locality name	Geographic coordinates	Locality code ¹	Collection year	N	A	N _P	H _{exp}	H _{obs}	Fis
Adriatic Sea	Ancona	44°12'N 13°15'E	AN ^M	2010	38	24	9	0.885	0.7746	0.138
	Bari	41°25'N 16°10'E	BA ^M	2010	42	23.8	8	0.8614	0.7483	0.143
Ionian Sea	Acitrezza	38°20'N 16°90'E	JO ^M	2010	39	25.4	7	0.8706	0.7576	0.143
		42°59'N								
Ligurian Sea	Elba	10°22'E 41°41'N	EN ^M	2010	40	23.8	3	0.8953	0.7763	0.146
Tyrrhenian Sea	Fiumicino	12°40'E 41°11'N	FM ^C	2010	40	24.6	4	0.8721	0.7838	0.114
	Gaeta	13°26'E 38°45'N	GA ^M	2010	32	22	6	0.867	0.7572	0.143
	Vibo Marina	16°80'E 40°84'N	VM ^C	2010	40	22.9	6	0.8644	0.7382	0.158
Sardinian Sea	Castel Sardo	08°34'E 40°32'N	SN ^M	2010	40	24.4	6	0.8825	0.7517	0.161
		08°11'E								
Sicilian Channel	Alghero	37°16'N 09°55'E	AL ^M	2010	39	23.7	6	0.8793	0.7622	0.146
	Bizerte (Tunisia)	35°11'N 12°70'E	BZ ^C	2009	40	24.2	3	0.8654	0.7678	0.125
	Lampedusa	33°24'N 11°13'E	LM ^C	2010	40	23.6	1	0.8745	0.7691	0.133
	Zarzis (Tunisia)		ZA ^C	2009	40	24.1	6	0.8824	0.8025	0.103

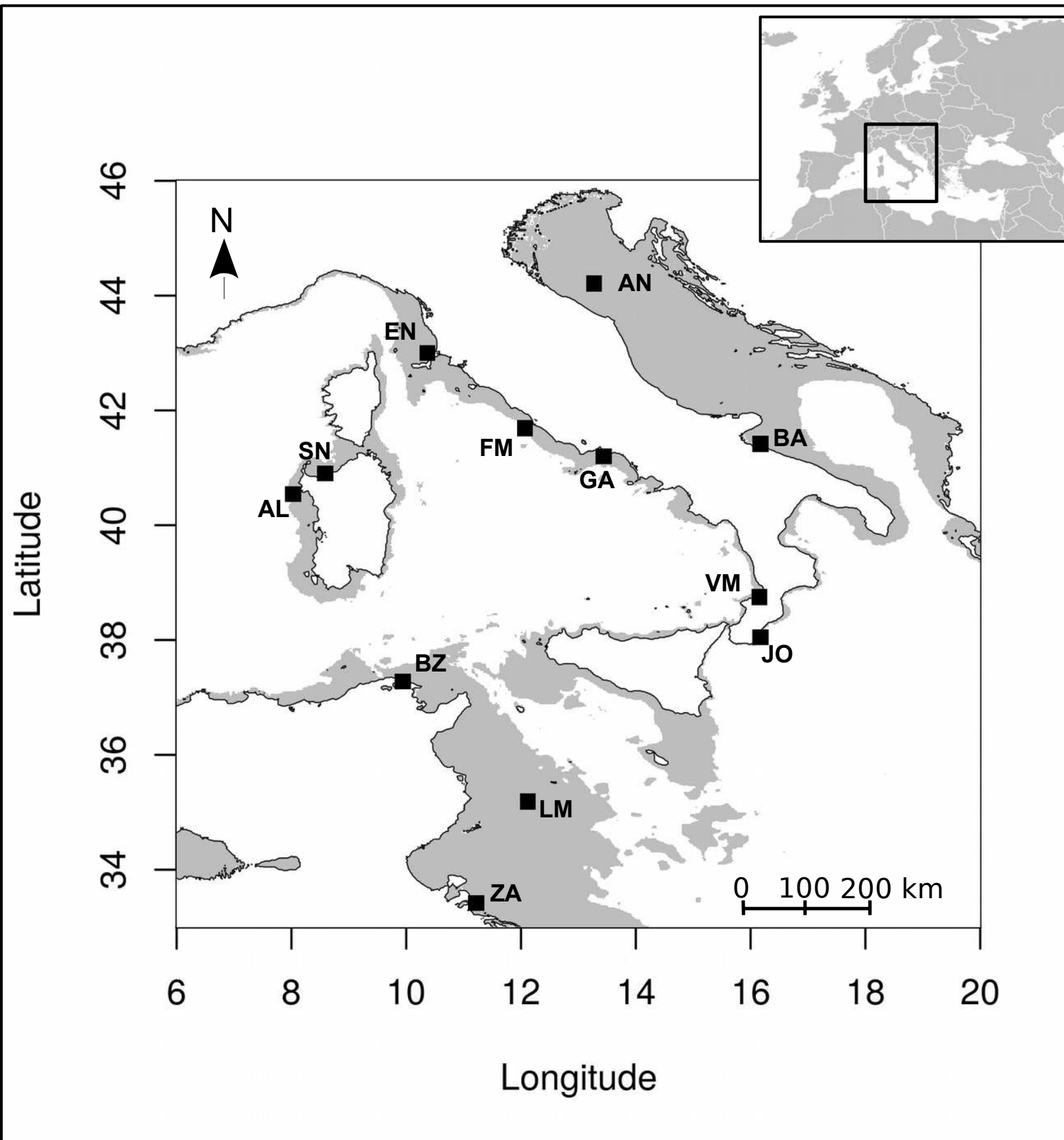
945

946 ¹ Superscript character indicate sampling source: M, MEDITS survey; C, commercial fishing

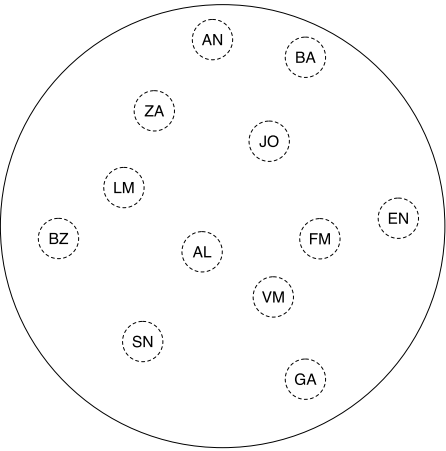
947 **Table 2** F_{ST} values (Weir & Cockerham 1984, below the diagonal) and R_{ST} (Slatkin, 1995;
948 above the diagonal) calculated for each pair of sampling locations. Significant values before
949 and after FDR correction are indicated underlined and bold respectively. For sample codes see
950 Table 1

	AN	BA	JO	EN	FM	GA	VM	SN	AL	BZ	LM	ZA
AN	-	<u>0.0194</u>	0.0016	0.0025	0.0014	0.0031	0.0067	0.002	0.0038	-0.0083	<u>0.0196</u>	0.0097
BA	<u>0.0092</u>	-	0.0066	<u>0.0169</u>	0.0091	<u>0.0377</u>	0.0115	0.0049	0.0112	0.007	0.0079	0.0097
JO	<u>0.0073</u>	<u>0.0055</u>	-	0.0054	-0.0001	0.0119	0.0001	-0.0016	-0.0077	-0.0051	0.0067	0.0055
EN	<u>0.0065</u>	<u>0.0064</u>	<u>0.0061</u>	-	-0.0078	0.0052	0.0017	-902	0.0135	0.0024	<u>0.0138</u>	<u>0.0125</u>
FM	<u>0.0055</u>	0.0041	0.0025	0.0024	-	0.0014	-0.0056	-0.008	0.0043	-0.0006	0.0108	<u>0.0131</u>
GA	0.0024	0.0032	0.0023	0.0041	0.0005	-	0.0072	0.0063	0.015	0.003	<u>0.0294</u>	<u>0.0332</u>
VM	<u>0.0075</u>	0.0013	0.0046	<u>0.0058</u>	0.0008	0.0018	-	-0.0007	0.0012	0.0051	<u>0.013</u>	0.0048
SN	<u>0.0063</u>	0.004	<u>0.0051</u>	0.0003	0.0033	0.0042	0.0051	-	0.0055	-195	0.0103	0.0098
AL	0.0039	0.0011	-0.0009	0.0044	0.0002	-0.0016	0.0003	<u>0.0059</u>	-	-0.0025	0.0135	0.0004
BZ	0.004	<u>0.0051</u>	0.003	<u>0.0072</u>	0.0029	0.0017	0.0037	<u>0.0063</u>	0.0005	-	0.0027	0.0036
LM	<u>0.0065</u>	0.0027	0.004	<u>0.0049</u>	0.0017	0.0016	0.0039	0.0041	0.0022	0.0039	-	0.0082
ZA	<u>0.0078</u>	0.0042	0.0022	<u>0.0067</u>	0.0037	<u>0.0057</u>	<u>0.006</u>	<u>0.0058</u>	0.0002	<u>0.0065</u>	<u>0.0058</u>	-

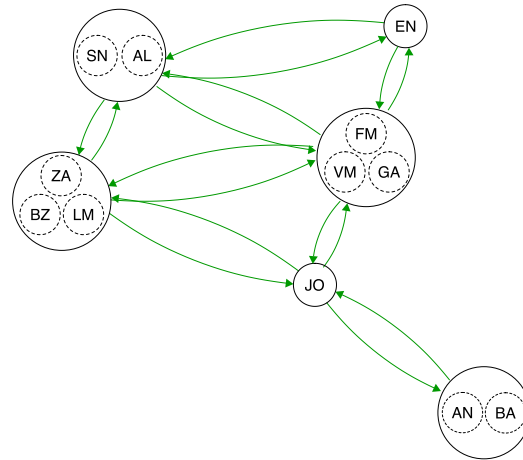
Figure 1



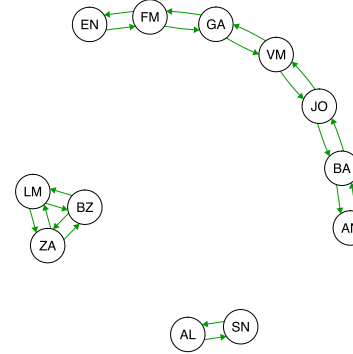
Model 0



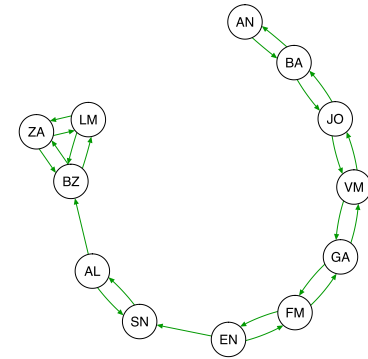
Model 1



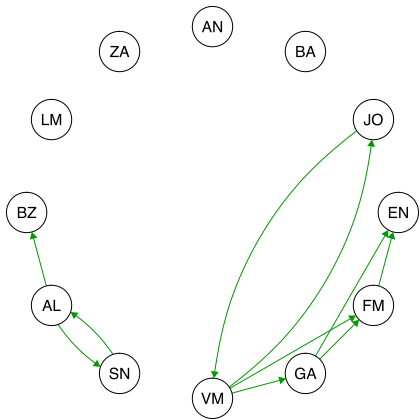
Model 2



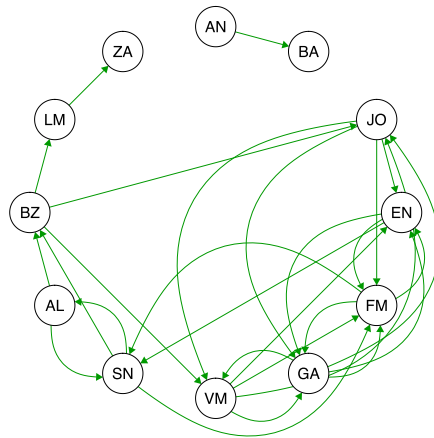
Model 3



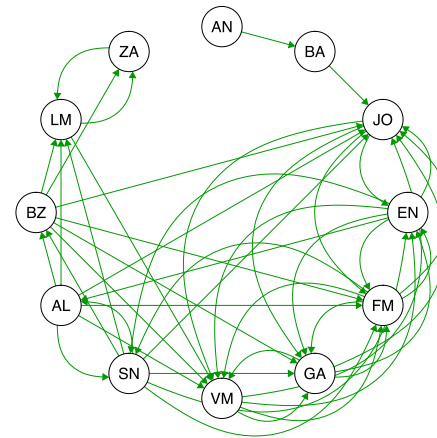
Model 4



Model 5



Model 6



Model 7

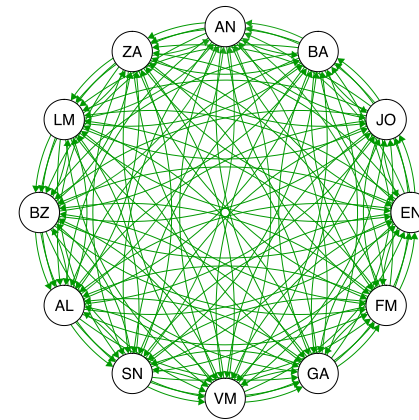
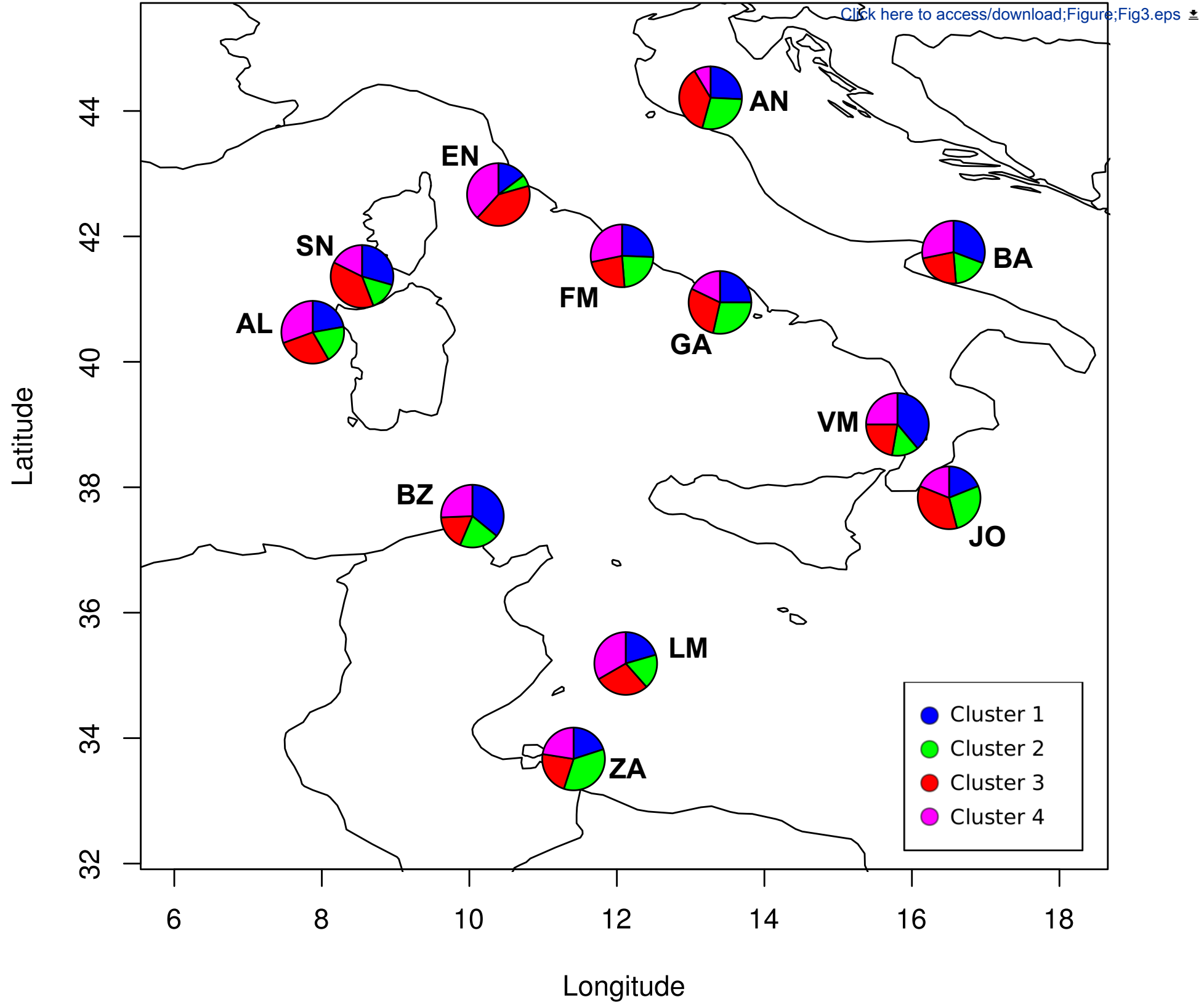
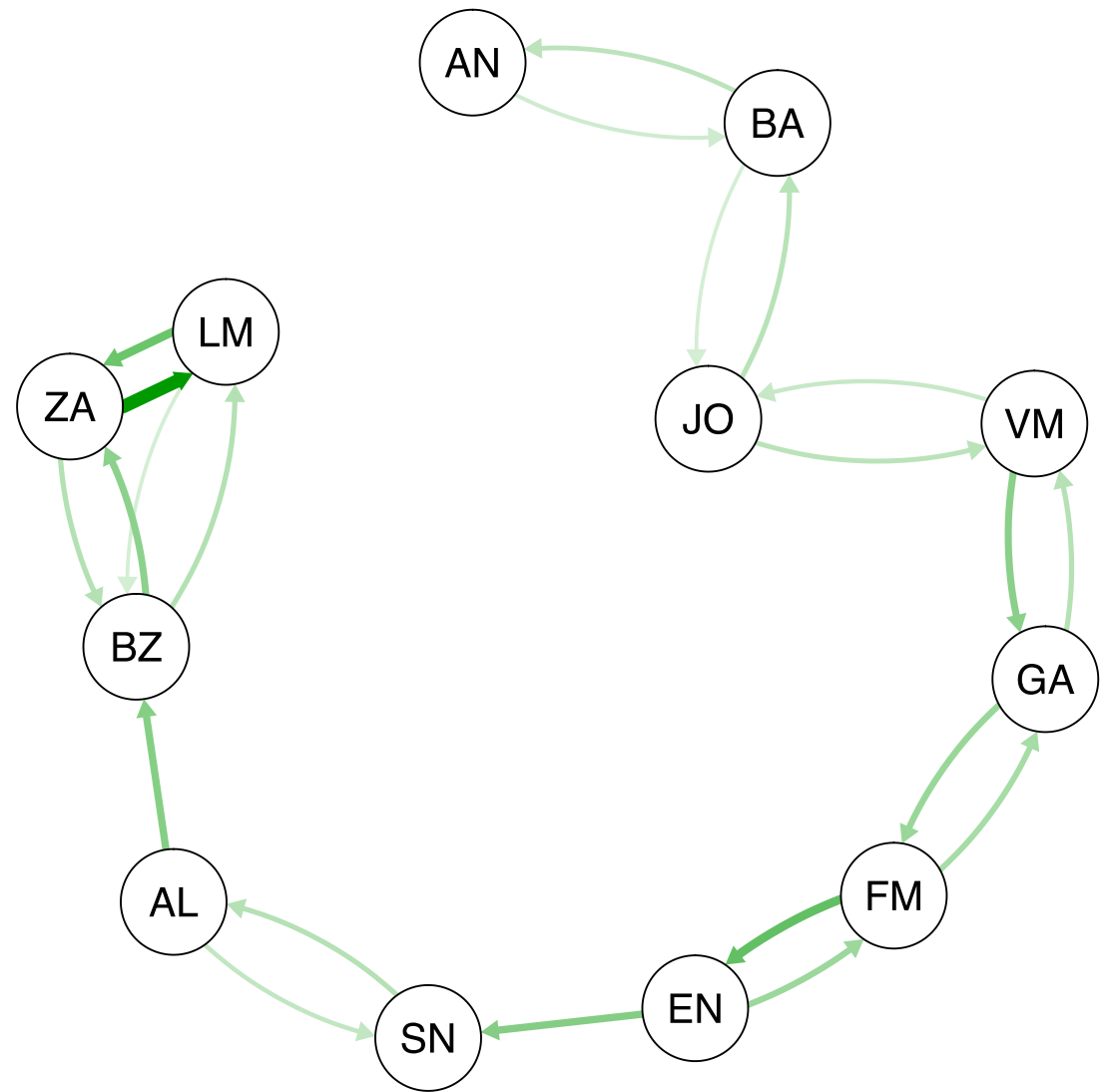


Figure 3



[Click here to access/download;Figure;Fig4.eps](#) 

b



Electronic Supplementary Material

Influence of hydrodynamic connectivity on the genetic structure and gene flow of the common pandora *Pagellus erythrinus*

Anna Rita Rossi, Paolo Colangelo, Léo Berline, Elisa Angiulli, Giandomenico Ardizzone, Chiheb Fassatoui, Luciana Sola

Online resource 1. Summary statistics for ten microsatellite loci over the twelve common pandora sampling sites analysed

Locus	N	K	Np	A	A _R	H _{WE}	Fis	Null All
MS2	467	83	11	35.6	33.16	High sign	0.272	0.131
MS3	465	43	13	15.7	14.25	High sign	0.183	0.075
MS4	465	42	6	25.4	23.46	High sign	0.092	0.043
MS6	468	14	3	6.4	6.11	0.0000	0.089	0.047
SL7	464	55	5	34.9	31.58	High sign	0.130	0.063
SL17	469	77	6	33	28.75	High sign	0.099	0.050
SL26	465	34	7	17.8	17.58	High sign	0.081	0.035
SL29	464	61	4	37.1	33.69	High sign	0.071	0.033
SL33	466	17	6	8.3	7.89	High sign	0.354	0.160
PbOviD102	466	38	4	22.6	22.60	0.0280	0.032	0.016

N = number of individuals, K = allele number, NP = number of private alleles, A = average number of allelels, AR = Allelic richness, HWE = significance deviation from the Hardy-Weinberg equilibrium, Fis = inbreeding coefficient; Null All = null alleles frequencies

Electronic Supplementary Material

Influence of hydrodynamic connectivity on the genetic structure and gene flow of the common pandora *Pagellus erythrinus*

Anna Rita Rossi, Paolo Colangelo, Léo Berline, Elisa Angiulli, Giandomenico Ardizzone, Chiheb Fassatoui, Luciana Sola

Online resource 2. Locus/site combination tests for null alleles (NA; in parentheses their estimated frequencies) and for stuttering errors (ST). In grey deviations from Hardy–Weinberg expectations

Locus	Locality											
	AN	BA	JO	EN	FM	GA	VM	SN	AL	BZ	LM	ZA
MS2	NA (0.18605)	NA (0.08541)	NA (0.09873)	NA (0.11984)	NA (0.09713)	NA (0.12473)	NA (0.15418)	NA (0.04502)	NA (0.12457)	NA (0.13913)	NA (0.16967)	NA (0.13864)
MS3	(0.01970)	(0.03759)	(0.05090)	(0.06050)	NA (0.12828)	NA/ST (0.13478)	(0.07617)	NA/ST (0.09982)	(0.07332)	(0.01328)	(0.09435)	(0.02852)
MS4	(0.06117)	(0.05013)	(0.01877)	(0.02947)	(0.05440)	(0.01664)	NA (0.07836)	(0.01451)	NA (0.06293)	(0.00000)	(0.00630)	(0.04910)
MS6	(0.00000)	(0.08305)	(0.00570)	(0.14292)	(0.00402)	(0.00000)	(0.13088)	(0.00465)	(0.09737)	(0.00000)	(0.00000)	(0.01637)
SL7	(0.03341)	NA (0.08705)	NA (0.07270)	(0.04892)	(0.06008)	NA (0.08435)	(0.03329)	NA (0.11093)	(0.03009)	NA (0.06539)	(0.04558)	(0.01979)
SL17	(0.02042)	(0.08967)	(0.10918)	(0.00063)	(0.00476)	(0.00334)	(0.06868)	(0.03620)	(0.06292)	(0.07935)	(0.06352)	(0.00000)
SL26	(0.04173)	(0.03611)	(0.03955)	NA (0.08419)	(0.00000)	(0.04894)	(0.00000)	(0.05848)	NA (0.07646)	(0.04591)	(0.00000)	(0.00000)
SL29	(0.02698)	(0.00000)	NA (0.06144)	(0.01355)	(0.00000)	(0.02539)	(0.00000)	(0.01637)	(0.04653)	NA (0.04492)	(0.03507)	(0.05382)
SL33	NA/ST (0.20935)	NA/ST (0.12897)	NA/ST (0.16804)	NA/ST (0.08890)	NA/ST (0.10385)	NA/ST (0.11962)	NA/ST (0.16804)	NA/ST (0.22001)	NA/ST (0.06403)	NA/ST (0.15800)	NA/ST (0.14429)	NA/ST (0.19752)
PbOviD102	(0.03193)	(0.02964)	(0.00018)	(0.00610)	(0.00000)	(0.00018)	(0.00646)	(0.05340)	(0.00000)	(0.00464)	(0.00000)	(0.00002)

Electronic Supplementary Material

Influence of hydrodynamic connectivity on the genetic structure and gene flow of the common pandora *Pagellus erythrinus*

Anna Rita Rossi, Paolo Colangelo, Léo Berline, Elisa Angiulli, Giandomenico Ardizzone, Chiheb Fassatoui, Luciana Sola

Online resource 3: POWSIM simulations to assess the statistical power of microsatellite loci to differentiate populations at varying levels of expected FST. Results of X2 and Fisher’s exact tests for the proportion of simulations out of 1000 significant with a critical value of 0.05.

Expected F_{ST}	N_e	t	χ^2 test (%)	Fisher’s test (%)
0.0005	1.000/ 5.000/ 10.000	1/ 5/ 10	49.7/ 52.7/ 50.5	47.5/ 50.3/ 49.3
0.0010	1.000/ 5.000/ 10.000	2/ 10/ 20	95.5/ 94.9/ 95.7	90.4/ 91.8/ 90.9
0.0025	1.000/ 5.000/ 10.000	5/ 25/ 50	100/ 100/ 100	100/ 100/ 100
0.0050	1.000/ 5.000/ 10.000	10/ 50/ 100	100/ 100/ 100	100/ 100/ 100
0.0100	1.000/ 5.000/ 10.000	20/ 100/ 200	100/ 100/ 100	100/ 100/ 100

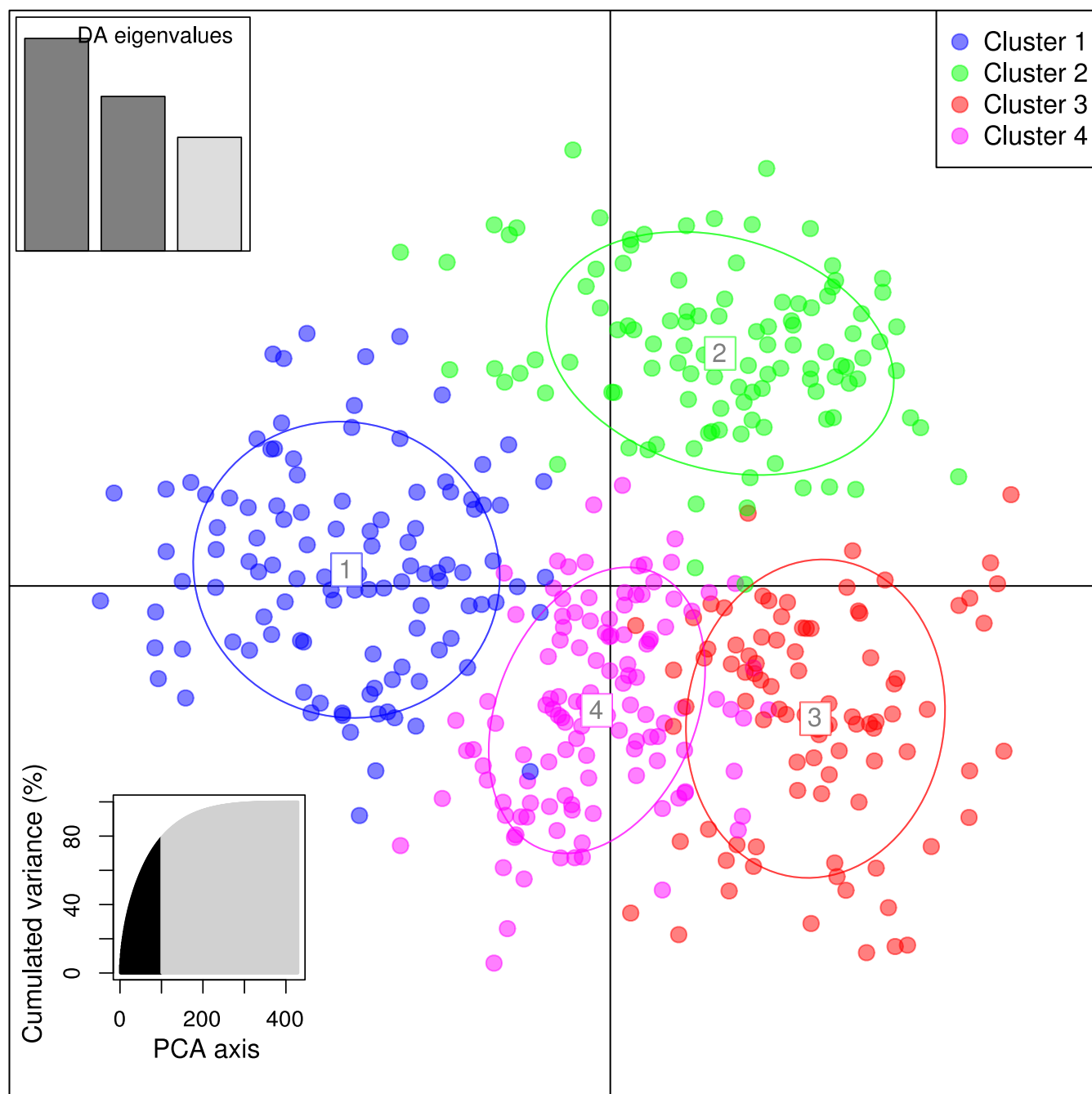
Influence of hydrodynamic connectivity on the genetic structure and gene flow of the common pandora *Pagellus erythrinus*

Anna Rita Rossi, Paolo Colangelo, Léo Berline, Elisa Angiulli, Giandomenico Ardizzone,

Chiheb Fassatoui, Luciana Sola

Online resource 4

Discriminant Analysis of Principal Component (DAPC). The obtained graph represents the individuals as dots and the groups (identify by k-means) as different colors. Eigenvalues of the discriminant axes (DA) and the cumulated variances of the PC axes used are displayed in insets.



Electronic Supplementary Material

Influence of hydrodynamic connectivity on the genetic structure and gene flow of the common pandora *Pagellus erythrinus*

Anna Rita Rossi, Paolo Colangelo, Léo Berline, Elisa Angiulli, Giandomenico Ardizzone, Chiheb Fassatoui, Luciana Sola

Online resource 5:

Mean connection time (MCT) among pair of sites. Only MCT below 200 days were considered. NaN indicates MCTs above 200 days

[illegible]

Electronic Supplementary Material

Influence of hydrodynamic connectivity on the genetic structure and gene flow of the common pandora *Pagellus erythrinus*

Anna Rita Rossi, Paolo Colangelo, Léo Berline, Elisa Angiulli, Giandomenico Ardizzone, Chiheb Fassatoui, Luciana Sola

Online resource 6: Model comparison of the eight models. For each model the marginal likelihood estimated using the Bezier approximation is reported. The probability of each model was calculated following Beerli and Palczewski (2010)

Model number	Bezier approximation	P model
Model 0	-7006182.17	0
Model 1	-546114.82	0
Model 2	-3788213.34	0
Model 3	-349000.46	1
Model 4	-3516744.21	0
Model 5	-1262798.92	0
Model 6	-442189.13	0
Model 7	-1218611.85	0